

Room-temperature pressureless bonding with silver nanowire paste: towards organic electronic and heat-sensitive functional devices packaging†

Peng Peng,^{ab} Anming Hu,^{*a} Hong Huang,^a Adrian P. Gerlich,^a Boxin Zhao^{bc} and Y. Norman Zhou^{*ab}

Received 30th March 2012, Accepted 5th May 2012

DOI: 10.1039/c2jm31979a

Heat-sensitive components packaging requires low temperature joining technology. The present study considers the feasibility of room-temperature pressureless joining of copper wires using silver nanowire paste. These joints achieve a tensile strength of 5.7 MPa and exhibit ultralow resistivity in the range of 101 nΩ m. An “*in situ* cleaning” action of PVP is proposed during the bonding process.

There are growing demands in the electronics industry for electrically conductive joints for device assembly while also striving to reduce the joining temperature due to the thermal sensitivity of components. This is a particular issue in the case of lead-free soldering^{1–6} where the general melting temperatures are in the range from 200 °C to 300 °C. This implies severe drawbacks for heat-sensitive substrates in organic electronic devices, such as flexible electronic book and organic light-emitting devices.^{7–11} Interconnects in ferroelectric materials with electrodes, especially for inorganic ferroelectric materials with low transition temperature or organic ferroelectric materials,^{12–15} also cannot be formed at such temperatures if they are close to their transition temperatures. Hence, a low temperature or even cold-interconnecting technique is required to minimize the temperature effects on the properties of heat-sensitive components during assembly. Low-pressure cold welding was developed to fabricate organic light-emitting devices^{16,17} and surface activated bonding has also been studied to interconnect electrodes for system packages.^{18–20} Some approaches benefit from nanotechnology, in which nanoscale diffusion bonding using metallic nanomaterials offers significant advantages over conventional soldering or adhesive bonding, such as lower bonding temperatures and higher diffusion rates.²¹ For example, low temperature interconnection processes using metallic

nanoparticle pastes, such as silver,^{22,23} copper²⁴ and gold,²⁵ appear to be a promising alternative for lead-free electronic packaging and flexible electronic interconnections.^{26,27} However, the required specific geometries and conditions of bonding surface, expensive equipment and external pressure for those methods are not feasible for practical applications.

Recently, efforts are being made to study the interconnecting of nanorods, nanowires, nanobelts and nanotubes, in order to further exploit the unique properties of these materials.^{28–33} For example, the welding of silver nanorods could form a zig-zag assembly,³⁴ cold welding of gold nanowires could be used to form next generation interconnects for dense logic circuits,⁸ and transparent electrodes were fabricated by joining silver nanowires (Ag NWs) on plastic films *via* mechanical pressing at room temperature.³⁵ However, to the authors' best knowledge, there is no report of the use of nanowires as a filler material to form a bonded joint. In this study, we present a novel pressureless room-temperature bonding process using silver nanowire paste.

Fig. 1 shows the microstructure of Ag NWs and the bonded samples where the highly concentrated paste exhibits a green-grayish colour. The Ag NWs are on average 13 μm in length and 60 nm in thickness, see Fig. 1a, with a pentagonal shape and 3 nm organic shells indicated in Fig. 1b. Fig. 1c–g shows the bonded joints between a Cu wire and another Cu wire, a silver-plated copper pad, a gold-plated polyimide pad, and a tin-doped indium oxide (ITO) coated polyethylene terephthalate (PET) substrate. The samples with flexible substrates also displayed low resistance even after folding. The influence of the polyvinylpyrrolidone (PVP) organic coating on the room-temperature bonding of copper wires using silver nanowires was systematically investigated.

It has been shown that the surface of Ag NWs may be free of organic coatings after washing with water, and this yields a reactive surface which readily allows Ag atom interdiffusion during sintering.³⁶ If the bare surfaces of the Ag NW are free of organics and come into contact there is a free path for surface diffusion and joint formation occurs because of a low activation energy and large driving force due to the reduction in surface energy. To study the effect of the washing process on the sintering behaviour of Ag NW paste, TGA testing was conducted at room-temperature up to 500 °C (with the washing process of the samples summarized in Fig. S1†). As washing times increase, the weight loss dramatically decreased from 20% for one washing cycle to only 0.4% for three cycles. A small fluctuation is evident on the derived weight change curves at 300 °C, which suggests

^aCentre for Advanced Materials Joining, Department of Mechanical and Mechatronics Engineering, University of Waterloo, 200 University Avenue West, Waterloo, ON, N2L 3G1, Canada. E-mail: a2hu@uwaterloo.ca; nzhou@uwaterloo.ca; Fax: +1 519 888-6197; Tel: +1 519 888-4567 ext. 35464

^bWaterloo Institute for Nanotechnology, University of Waterloo, 200 University Avenue West, Waterloo, ON, N2L 3G1, Canada

^cDepartment of Chemical Engineering, University of Waterloo, 200 University Avenue West, Waterloo, ON, N2L 3G1, Canada

† Electronic supplementary information (ESI) available: Washing cycles effect on organic contents of AgNW pastes. Sintering behaviours of pastes with different washing times. Bonding and testing configurations. Interface of joints bonded at room-temperature. EDX results for the interface. See DOI: 10.1039/c2jm31979a

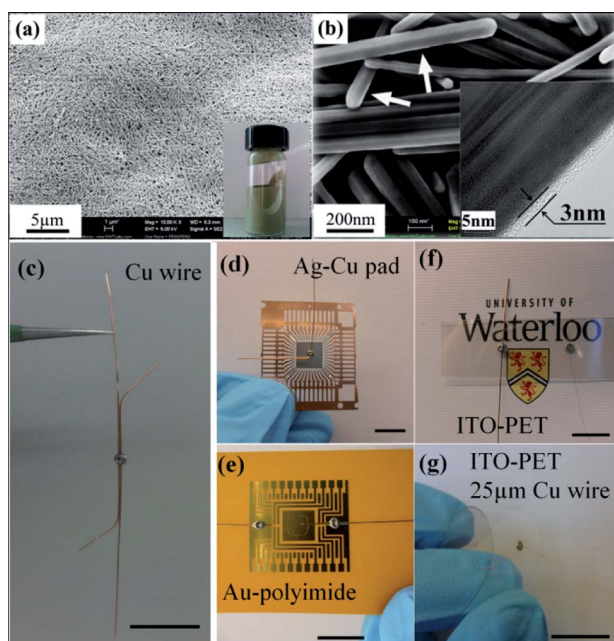


Fig. 1 (a) SEM image of as-centrifuged Ag NW paste (inset photo is the greenish-grey paste). (b) SEM image of pentagon-shaped (as arrows indicate) Ag NW with 60 nm mean thickness. Inset TEM image displayed the organic coating on the side of Ag NW. Optical images of 250 μm copper wires bonded with (c) copper wire, (d) silver coated copper pad, (e) gold coated polyimide and (f) ITO plated PET. (g) 25 μm copper wire bonded on flexible ITO-PET. (c-g, scale bar = 10 mm).

the organics were readily removed almost without residuals. The as-synthesized paste could be stored for half a year and no precipitate was observed. However, when washed 3 times the pastes began to precipitate after sitting for three weeks. If the Ag NW paste is washed twice, it is quite stable and only partial joining of nanowires was observed even upon heating at 100 $^{\circ}\text{C}$ for 1 hour (see Fig. S2† summarizing the sintering of pastes). The fresh paste washed 3 times exhibited an unsintered morphology, whereas it started to interconnect at room-temperature and form three-dimensional networks after three weeks, in which the networks became further sintered at a higher working temperature which provided high strength.²⁶ If the paste was heated at 200 $^{\circ}\text{C}$ for 1 hour, the Ag NWs grew thinner or coarser, and heating to 300 $^{\circ}\text{C}$ for 1 hour resulted in the formation of particles. It is worth it to mention that paste which was washed for three cycles was prone to agglomeration and setting after three weeks but still worked for bonding after sonication. If continually stored for half a year, the paste will completely precipitate and cannot be used for bonding. Therefore, it is speculated that the three-time washed paste's pot life is around six months. However, those pastes washed with one or two cycles could be stored for more than half a year in practical applications.

A plot of the joint strength of bonded samples as a function of bonding temperature using washed paste following pressureless bonding is shown in Fig. 2a (see Fig. S3† for bonding and testing configurations). The sample bonded at 60 $^{\circ}\text{C}$ using paste following one washing cycle resulted in poor strength. With increased washing times the bonding strength increased significantly due to the removal of organics from the interface of the Ag NWs, since the organics hamper the sintering process by limiting Ag atom interdiffusion. Two

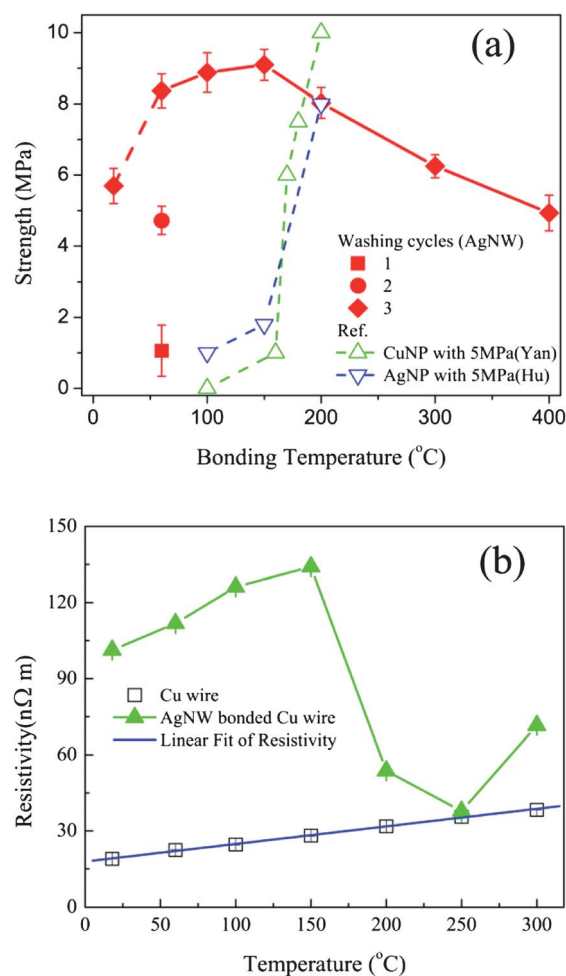


Fig. 2 (a) Tensile shear strength of bonded Cu-Cu wires with Ag NW paste as a function of bonding temperature, the pastes washed once and twice for bonding were compared (data of Cu NP are from Yan's paper²⁴ and data of Ag NP are from Hu's paper²⁶). (b) Resistivity of bonded Cu wire joint with Ag NW paste washed three times as a function of sintering and testing temperatures. Bulk resistivity of pure Cu wire was compared.

Cu wires were bonded at room-temperature to achieve a joint strength of 5.7 ± 0.5 MPa when 3 paste washing cycles were employed. The interface of cross-section for the joint was very sharp with continuous bonding (see Fig. S4† for interface of joints bonded at room-temperature), similar to joints bonded using Ag nanoparticle (NP) paste,²⁷ however the structure of filler material was not porous as in the case of Ag metallo-organic NPs.²² Comparing with the other published works, Cu NP²⁴ and Ag NP²⁶ begins to bond only when the temperatures reach 150 $^{\circ}\text{C}$, resulting in strengths of 1 to 2 MPa when a 5 MPa bonding pressure is applied because the nanoparticles need to be sintered first and then form networks for bonding.³⁶⁻³⁸ Herein, it is believed that the washed nanowires have interconnected and formed networks during bonding at room-temperature or with the application of moderate (<150 $^{\circ}\text{C}$) temperatures. Due to the more intense sintering of Ag NWs which occurs at higher temperatures, the strength increased to 9.1 ± 0.4 MPa when the temperature increased to 150 $^{\circ}\text{C}$, which is a higher strength than joints bonded with Cu NP and Ag NP using 5 MPa of pressure.^{24,26} The strength decreased as bonding temperature further increased, due to the aforementioned break-up of Ag NWs at high temperature (see Fig. S2e†).

The effects of PVP have been minimized in the present study through the application of repeated water washing in order to achieve bonding at room-temperature. In addition, this promoted high conductivity as a secondary benefit from PVP removal. As shown in Fig. 2b, the room-temperature bonded Cu wire joints exhibited ultralow resistivity ($101.27 \pm 0.05 \text{ n}\Omega \text{ m}$) because of the metallic bonding of Cu–Ag and Ag NW–NW. This value is two orders of magnitude lower than the value reported for a Cu NPs joint ($8 \times 10^4 \text{ n}\Omega \text{ m}$), and similar to that obtained after prolonged times in cured and reflowed Ag nanocomposites ($60 \text{ n}\Omega \text{ m}$).^{24,39} For comparison, the resistivity of the Cu wire was plotted, which presents a linear relationship with temperature because of the temperature coefficient of resistance.⁴⁰ This coefficient accounts for the slight increasing of resistivity of a bonded joint from 18°C to 150°C . The further sintering of the Ag NWs at elevated temperatures results in the enhancement of conductivity. At 250°C , the joint obtained the lowest resistivity $37.83 \pm 0.04 \text{ n}\Omega \text{ m}$ which is comparable with $35.58 \pm 0.12 \text{ n}\Omega \text{ m}$ observed for a pure Cu wire. However, because of broken nanowires and oxidation of Cu after 250°C , increased temperature introduced the increasing of resistivity.

The fracture surfaces of bonded samples before and after testing have been observed to investigate the joining behaviour of Ag NW pastes. At room-temperature, the pristine sample depicts the straight Ag NWs well interconnected and formed three-dimensional Ag networks aforementioned in Fig. 3a. In TEM images in Fig. 3b, the Ag NWs are bonded together through either end-to-end, end-to-side, or a side-to-side manner. The inset image illustrates the tri-terminal junction formed by Ag NWs. After testing, interconnected Ag NWs were broken with obvious deformation and necking as highlighted with circles in Fig. 3c. And the AgNWs were distorted because of the strain under loading which indicates the AgNW networks are ductile. This high strength of nanowires due to the nano-scale effects⁴¹ and the good ductility of networks accounts for the fracture strength of bonded joints. However, at high bonding temperature, Ag NWs transformed into particles and the failure points of filler materials were difficult to identify (see Fig. 3d).

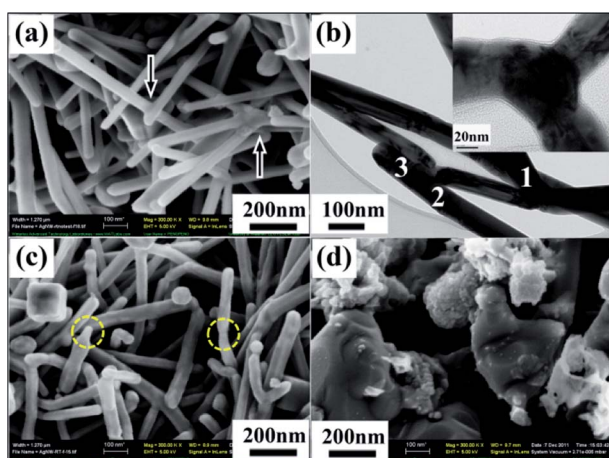


Fig. 3 SEM (a) and TEM (b) images of three-dimensional Ag networks formed at room-temperature. Arrows indicating the Ag–Ag junctions, numbers 1, 2 and 3 showing end-to-end, end-to side and side-to-side three different bonding modes of Ag NWs, inset is the tri-terminal junction. Fracture surfaces on bonded samples bonding at (c) room-temperature and (d) 300°C . Circles indicate the necking of Ag NWs during failure.

It is interesting to note that the Cu wire fracture surface of a joint bonded at room-temperature was covered by a residual thin layer of Ag NW after testing as shown in Fig. 4a. This indicates that the fracture of the joint is not in the interface of Cu–Ag, but rather the Ag NW networks close to the Cu interface. The high-magnification SEM images of an Ag network matrix are depicted in Fig. 4b showing 100% pure Ag in EDX results. Some particles mixed with and grew on Ag NWs which are in the folded thin layer in Fig. 4c and on the Cu surface in Fig. 4d. This thin layer contains 18 at.% of O and 20 at.% Cu (see Fig. 4c) while the Cu surface is 23 at.% O in Fig. 4d. Therefore, the particles were CuO which originated from the oxidation of Cu on the surface. Those CuO nanoparticles might be from the Cu surface because of incomplete cleaning or oxidation of Cu during bonding. However, those nanoparticles dramatically decreased on the Cu surface when bonding temperatures increased to 100°C , see Fig. 4e. If the bonding temperatures continue to increase to 150°C , no CuO particles are observed, but only well interconnected Ag NWs appear on the Cu surface, see Fig. 4f. Here, one should consider that the bonds of the PVP could be terminated with hydroxyl groups due to the presence of hydrogen peroxide and water in polymerization during the fabrication process.⁴² Hence, PVP can be used as not only a stabilizer but also as a reducing agent⁴³ as it has been successfully used to synthesized noble metal nanomaterials.^{44–46} It is believed that the residual PVP could prevent the formation of CuO and/or deoxidize CuO to Cu and further clean the Cu–Ag interface to provide better conditions for interdiffusion and bonding. This “*in situ* cleaning” hypothesis is proposed as follows: hydroxyl groups terminated PVP reacts with copper oxide and generates

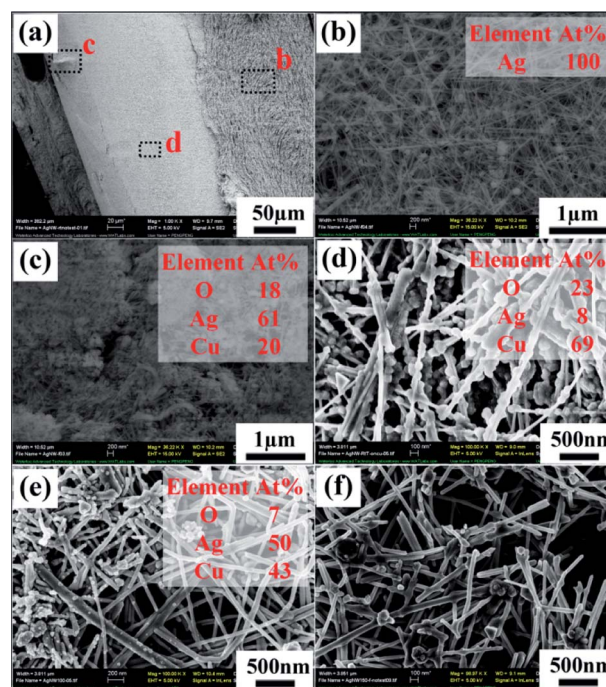


Fig. 4 SEM images of (a) failure joint bonded at room-temperature, the high-magnification images of squares corresponding to (b) Ag matrix surface, (c) folded Ag NW layer, with particles attached on AgNW and (d) Cu wire surface with EDX results. The Cu wire surface of failure joint bonded at (e) 100°C and (f) 150°C . (Fig. S5† shows the detailed EDX results).

copper for the “*in situ* cleaning” process during bonding or preventing the formation of copper oxide (Scheme 1).

To study the bonding behaviours of Ag NW with Cu, CuO and Ag NW at room-temperature, TEM was employed to observe the cross-sections of bonded samples. Fig. 5a, Ag NW bonded on the Cu surface and the (111) plane of Ag and (200) of Cu well matched and formed a metallic bond, see Fig. 5b, similar to that observed when using Ag nanoparticle paste as the bonding material^{22,26,27} and connected with CuO particles. Fig. 5c depicts the end-to-end interconnect of Ag NWs and the square area corresponding to Fig. 5d. The distances of lattice fringes are 2.32 Å and 1.96 Å in agreement with (111) and (200) planes of silver.^{47,48} The clear metallic bonding at the atomic level accounts for the good bond strength and conductivity observed during testing. In addition, the presence of CuO might serve as a beneficial co-bonding material in local areas during the room-temperature bonding and contribute to the good mechanical properties of joints.

In summary, room-temperature interconnection of copper wires with good tensile shear strength and conductivity has been achieved by AgNW paste without bonding pressure. Organic compounds could be removed from the surfaces of AgNW, leaving the surface of the nanowires largely free of PVP coating and activated for bonding. The residual PVP could prevent the formation of CuO and promote bonding by “*in situ* cleaning” behaviour. The NW can form a metallic bond with the copper surface, and with adjacent AgNWs through



Scheme 1 “*In situ* cleaning” behaviour of PVP during bonding.

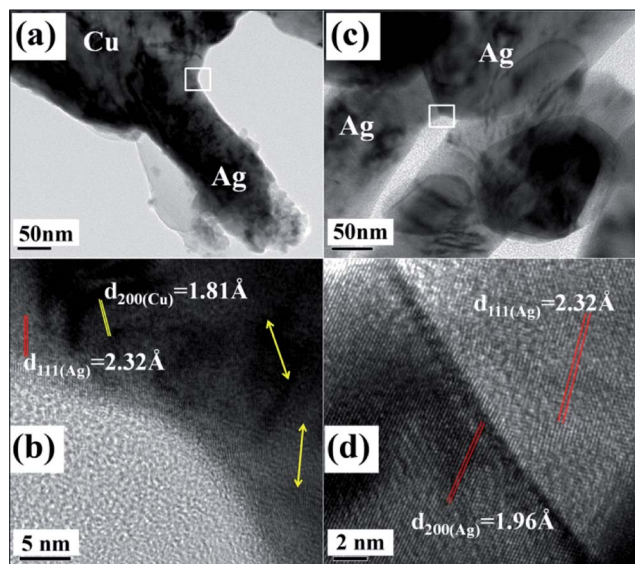


Fig. 5 TEM images of cross-section of room-temperature bonded joint. (a) Cu–Ag interface and corresponding high-resolution image; (b) lattice fringe images showing the (111) plane of Ag and (200) of Cu well matched (arrows indicate the lattice directions of polycrystalline Cu). The interface of two AgNWs (c) with end-to-end bonding and square area corresponding to the high-resolution image; (d) two different planes of each wire $d_{200} = 1.96$ Å and $d_{111} = 2.32$ Å.

end-to-end, end-to-side and side-to-side manners. The failure of AgNWs accounts for the fracture of bonding joints. This room-temperature pressureless technique has potential applications for heat-sensitive component assembling and/or microelectronics packaging. Furthermore, “*in situ* cleaning” by removal of PVP and oxide could be adopted for bonding of oxidized components.

Experimental

Bonding using silver nanowire paste

Ag NWs were prepared in a polyol solution with polyvinylpyrrolidone (PVP) as a structure directing reagent using a method modified from the literature.^{49,50} Ag NWs were washed by deionized (DI) water to remove the ethylene glycol and PVP and condensed by centrifugation. Prior to bonding, the copper wires with 0.25 mm thickness were cut into 60 mm pieces and ultrasonically cleaned in acetone for 3 minutes to remove the organics, diluted HNO_3 for 1 minute to remove the oxide layer and rinsed in ultrapure water (electrical resistivity approximately 18 MΩ cm). A fine needle attached to a 10 ml syringe was used to locate the Ag nanopaste between two clean copper wires (shown in Fig. S1a†). After depositing 0.05 ml highly concentrated Ag nanopaste, the assembly of copper wires and paste was put at room-temperature (18 °C) or heated at 60–200 °C in air for 1 hour without bonding pressure.

Testing of bonded joints

Tensile shear testing was conducted by loading the wires in the axial direction at a rate of 0.5 mm min^{−1} using a microtensile tester (Instron 5548). A field-emission scanning electron microscope (LEO 1530 FE-SEM) was used to study the microstructure of interfaces and fracture surfaces of bonded samples. Energy-dispersive X-ray spectroscopy (EDX, EDAX Pegasus 1200) was employed for elemental analysis. Interfaces of room-temperature bonded samples produced with Ag NW paste which was washed three times were characterized by observing the cross-section using transmission electron microscopy (TEM, PHILIPS CM12) and high resolution transmission electron microscopy (HRTEM, JEOL 2010F). Resistivity of joint, ρ , was calculated using $\rho = A \times R/l$, where resistance (R) was measured by a four probes low resistance Ohmmeter (DUCTER DLRO 10X), A and l are area of section and length.

Acknowledgements

Support from the Canadian Research Chairs (CRC) program, National Sciences and Engineering Research Council (NSERC) and the State Scholarship Fund of China (no. 2010640009) are greatly acknowledged. We thank the comments and suggestions of Dr Xiaogang Li, Dr Lei Liu and Prof. Scott Lawson from the Centre for Advanced Materials Joining at the University of Waterloo, and Mr Fred Pearson from Canadian Center for Electron Microscopy, McMaster University for help with TEM observation.

Notes and references

- 1 Y. Li, K. Moon and C. P. Wong, *Science*, 2005, **308**, 1419.
- 2 K. Tu, A. Gusak and M. Li, *J. Appl. Phys.*, 2003, **93**, 1335.
- 3 K. Saganuma, *Curr. Opin. Solid State Mater. Sci.*, 2001, **5**, 5.
- 4 J. Glazer, *Int. Mater. Rev.*, 1995, **40**, 65.
- 5 D. R. Frear and P. T. Vianco, *Metall. Mater. Trans. A*, 1994, **25**, 1509.

- 6 J. P. Coughlin, J. J. Williams, G. A. Crawford and N. Chawla, *Metall. Mater. Trans. A*, 2009, **40**, 176.
- 7 K. Zeng and K. N. Tu, *Mater. Sci. Eng., R*, 2002, **38**, 55.
- 8 Y. Lu, J. Y. Huang, C. Wang, S. Sun and J. Lou, *Nat. Nanotechnol.*, 2010, **5**, 218.
- 9 Q. Cui, F. Gao, S. Mukherjee and Z. Gu, *Small*, 2009, **5**, 1246.
- 10 L. Hu, M. Pasta, F. L. Mantia, L. Cui, S. Jeong, H. D. Deshazer, J. W. Choi, S. M. Han and Y. Cui, *Nano Lett.*, 2010, **10**, 708.
- 11 X. Zeng, Q. Zhang, R. Yu and C. Lu, *Adv. Mater.*, 2010, **22**, 4484.
- 12 D. Damjanovic, in *The Science of Hysteresis*, Elsevier, 2006, ch. 4, p. 344.
- 13 P. Ravindran, A. Delin, B. Johansson and O. Eriksson, *Phys. Rev. B: Condens. Matter*, 1999, **59**, 1776.
- 14 K. T. Ko, M. H. Jung, Q. He, J. H. Lee, C. S. Woo, K. Chu, J. Seidel, B. G. Jeon, Y. S. Oh, K. H. Kim, W. I. Liang, H. J. Chen, Y. H. Chu, Y. H. Jeong, R. Ramesh, J. H. Park and C. H. Yang, *Nat. Commun.*, 2011, **2**, 567.
- 15 S. Horiuchi and Y. Tokura, *Nat. Mater.*, 2008, **7**, 357.
- 16 C. Kim, P. E. Burrows and S. R. Forrest, *Science*, 2000, **288**, 831.
- 17 C. Kim and S. R. Forrest, *Adv. Mater.*, 2003, **15**, 541.
- 18 A. Shigetou, T. Itoh, K. Sawada and T. Suga, *IEEE ECTC*, 2008, vol. 27–30, p. 1405.
- 19 M. M. R. Howlader, A. Yamauchi and T. Suga, *J. Micromech. Microeng.*, 2011, **21**, 025009.
- 20 N. Watanabe and T. Asano, *IEEE ECTC*, 2010, vol. 1–4, p. 1763.
- 21 Y. Zhou, in *Microjoining & Nanojoining*, Woodhead, CRC, England, 2008, ch. 25, p. 749.
- 22 E. Ide, S. Angata, A. Hirose and K. F. Kobayashi, *Acta Mater.*, 2005, **53**, 2385.
- 23 J. G. Bai, Z. Z. Zhang, J. N. Calata and G. Q. Lu, *IEEE Trans. Compon. Packag. Technol.*, 2006, **29**, 589.
- 24 J. Yan, G. Zou, A. Hu and Y. Zhou, *J. Mater. Chem.*, 2011, **21**, 15981.
- 25 T. Bakhishev and V. Subramanian, *J. Electron. Mater.*, 2009, **38**, 2720.
- 26 A. Hu, J. Y. Guo, H. Alarifi, G. Patane, Y. Zhou, G. Compagnini and C. X. Xu, *Appl. Phys. Lett.*, 2010, **97**, 153117.
- 27 H. Alarifi, A. Hu, M. Yavuz and Y. Zhou, *J. Electron. Mater.*, 2011, **40**, 1394.
- 28 X. Li, F. Gao and Z. Gu, *Open Surf. Sci. J.*, 2011, **3**, 91.
- 29 A. R. Madaria, A. Kumar, F. N. Ishikawa and C. Zhou, *Nano Res.*, 2010, **3**, 564.
- 30 P. X. Gao, C. S. Lao, W. L. Hughes and Z. L. Wang, *Chem. Phys. Lett.*, 2005, **408**, 174.
- 31 Z. X. Zhang, X. Y. Chen and F. Xiao, *J. Adhes. Sci. Technol.*, 2011, **25**, 1465.
- 32 G. G. Yadav, G. Zhang, B. Qiu, J. A. Susoreny, X. Ruan and Y. Wu, *Nanoscale*, 2011, **3**, 4078.
- 33 Y. Zhang and H. Dai, *Appl. Phys. Lett.*, 2000, **77**, 3015.
- 34 D. Chen and L. Gao, *J. Cryst. Growth*, 2004, **264**, 216.
- 35 T. Tokuno, M. Nogi, M. Karakawa, J. Jiu, T. T. Nge, Y. Aso and K. Suganum, *Nano Res.*, 2011, **4**, 1215.
- 36 S. Magdassi, M. Grouchko, O. Berezin and A. Kamyshny, *ACS Nano*, 2010, **4**, 1943.
- 37 K. Moon, H. Dong, R. Maric, S. Pothukuchi, A. Hunt, Y. Li and C. P. Wong, *J. Electron. Mater.*, 2005, **34**, 168.
- 38 R. Zhang, K. Moon, W. Li and C. P. Wong, *J. Mater. Chem.*, 2010, **20**, 2018.
- 39 H. Jiang, K. Moon, Y. Li and C. P. Wong, *Chem. Mater.*, 2006, **18**, 2969.
- 40 W. Steinhögl, G. Schindler, G. Steinlesberger, M. Traving and M. Engelhardt, *J. Appl. Phys.*, 2005, **97**, 023706.
- 41 A. M. Leach, M. McDowell and K. Gall, *Adv. Funct. Mater.*, 2007, **17**, 43.
- 42 K. Raith, A. V. Kühn, F. Rosche, R. Wolf and R. H. H. Neubert, *Pharm. Res.*, 2002, **19**, 556.
- 43 Y. Xiong, I. Washio, J. Chen, H. Cai, Z. Y. Li and Y. Xia, *Langmuir*, 2006, **22**, 8563.
- 44 C. E. Hoppe, M. Lazzari, I. Pardiñas-Blanco and M. A. López-Quintela, *Langmuir*, 2006, **22**, 7027.
- 45 Y. Zhan, Y. Lu, C. Peng and J. Lou, *J. Cryst. Growth*, 2011, **325**, 76.
- 46 H. Wang, X. Qiao, J. Chen, X. Wang and S. Ding, *Mater. Chem. Phys.*, 2005, **94**, 449.
- 47 X. C. Jiang, S. X. Xiong, Z. A. Tian, C. Y. Chen, W. M. Chen and A. B. Yu, *J. Phys. Chem. C*, 2011, **115**, 1800.
- 48 E. A. Owen and G. I. Williams, *J. Sci. Instrum.*, 1954, **31**, 49.
- 49 Y. Sun, B. Gates, B. Mayers and Y. Xia, *Nano Lett.*, 2002, **2**, 165.
- 50 Y. Sun and Y. Xia, *Adv. Mater.*, 2002, **14**, 833.